

2018-04-15

A comparison of ground-based methods for estimating canopy closure for use in phenology research

Smith, AM

<http://hdl.handle.net/10026.1/10822>

10.1016/j.agrformet.2018.01.002

Agricultural and Forest Meteorology

Elsevier Masson

All content in PEARL is protected by copyright law. Author manuscripts are made available in accordance with publisher policies. Please cite only the published version using the details provided on the item record or document. In the absence of an open licence (e.g. Creative Commons), permissions for further reuse of content should be sought from the publisher or author.

1 **A comparison of ground-based methods for**
2 **estimating canopy closure for use in phenology**
3 **research**

4
5 **Alison M. Smith^{1,*} & Paul M. Ramsay¹**
6 ¹School of Biological and Marine Sciences, University of Plymouth, Plymouth, PL4 8AA,
7 UK

8 ***Corresponding author:** School of Biological and Marine Sciences, University of
9 Plymouth, Plymouth, PL4 8AA, UK; alison.smith@plymouth.ac.uk; tel. +44-1752-
10 584600.

11 Key words: phenology, canopy openness, hemispherical photography, fisheye
12 photography, citizen science

13

14 **A comparison of ground-based methods for
15 estimating canopy closure for use in phenology
16 research**

17

18 **Abstract**

19 Climate change is influencing tree phenology, causing earlier and more prolonged
20 canopy closure in temperate forests. Canopy closure is closely associated with
21 understorey light, so shifts in its timing have wide-reaching consequences for ecological
22 processes in the understorey. Widespread monitoring of forest canopies through time is
23 needed to understand changes in light availability during spring in particular. Canopy
24 openness, derived from hemispherical photography, has frequently been used as a
25 proxy for understorey light. However, hemispherical photography is relatively resource
26 intensive, so we tested a range of inexpensive alternatives for monitoring variability in
27 canopy closure (visual estimation, canopy scope, smartphone photography, smartphone
28 photography with fisheye attachment; and image analysis with specialist hemispherical
29 photography software or with simpler, open access image analysis software).
30 Smartphone photography with an inexpensive fisheye lens attachment proved the most
31 reliable estimator of canopy closure. We found no significant difference in canopy
32 estimations from three widely-owned smartphone models with differing resolutions and
33 fields of view, and no significant effect of camera operator on the results. ImageJ, a free
34 image analysis software, detected canopy variability in a similar way to HemiView
35 specialist hemispherical photography software. We recommend a combination of
36 smartphone photography with fisheye attachment and analysis with ImageJ for
37 identifying changes in the timing of canopy closure (but not for estimating absolute
38 canopy closure). We discuss how large-scale citizen science using this approach could
39 generate meaningful and comparative data on the timings of canopy closure in different
40 forests, year-to-year.

41

42 1. Introduction

43 Climate change is affecting forest ecosystems around the globe, with changes in tree
44 phenology widely documented for temperate forests (Richardson et al., 2013; Roberts
45 et al., 2015; Vitasse et al., 2011). Growing season extensions have been observed for
46 many European tree species, most notably due to canopies coming into leaf earlier
47 (Menzel and Fabian, 1999; Menzel et al., 2006; Thompson and Clark, 2008). The
48 phenology of dominant canopy trees exerts strong influence on the understorey
49 environment, as canopy openness is highly related to available photosynthetically active
50 radiation (PAR) (Brusa and Bunker, 2014; Gonsamo et al., 2013; Promis et al., 2012),
51 influencing microclimate, soil respiration (Giasson et al., 2013; Yuste et al., 2004) and
52 understorey plant dynamics (Van Couwenberghe et al., 2011). Therefore, earlier canopy
53 closure and later senescence is likely to have wide-ranging impacts on the phenology
54 and life processes of understorey plants and wider forest biodiversity. Studies have
55 indicated threats to spring ephemeral herbs that utilise the period before canopy closure
56 for completing their life cycle (Kim et al., 2015). Many tree saplings depend on spring
57 sunlight prior to canopy closure for their growth and survival (Augsburger, 2008).
58 Understorey species that are shade tolerant or those with greater phenological plasticity
59 are likely to gain competitive advantage (De Frenne et al., 2011), and invasive species
60 could become more prevalent (Engelhardt and Anderson, 2011; Willis et al., 2010). As
61 canopy openness is a key determinant of ecological processes in the understorey,
62 effective methods for monitoring intra and inter-annual changes in the timing of canopy
63 closure/openness would be very useful, especially if they allowed data to be collected
64 across a variety of spatial scales, and with plenty of replication.

65 Canopy phenology has been extensively studied in recent years. Satellite remote
66 sensing has enabled data collection of forest leaf phenology at large spatial scales
67 (Boyd et al., 2011; Wang et al., 2016; White et al., 2009; Wu and Liu, 2013; Zhang et
68 al., 2005). These methods focus on deriving estimates of canopy green-up dates from
69 Normalised Difference Vegetation Index (NDVI) or Enhanced Vegetation Index (EVI)
70 data, for the purpose of tracking photosynthetic activity to assess forest productivity, gas
71 exchange and phenological feedbacks to the climate system (Richardson et al., 2013).
72 While remote sensing data is useful for identifying large-scale phenological trends, the
73 coarse resolution means that local variations between forest stands are often masked
74 (Fisher et al., 2006; White et al., 2014). Furthermore, loss of temporal resolution due to

75 atmospheric conditions (Cleland et al., 2007; White et al., 2014), and difficulties
76 separating greening of the understorey from canopy greening (Hamunyela et al., 2013),
77 can compromise the use of this data for identifying shifts in canopy closure timing.

78 A range of ground-based methods have been used to assess canopy structure and
79 understorey light environments at the forest-level. Direct measures of understorey light
80 are highly affected by sky conditions and accurate determination requires continuous
81 measurement over several days (Engelbrecht and Herz, 2001; Gendron et al., 1998). This
82 makes direct measurements inappropriate for phenology studies where the objective is
83 to assess variation through time. As an alternative, hemispherical photography and Plant
84 Canopy Analysers (PCAs) such as the LAI-2200, are commonly used to assess structural
85 attributes of forest canopies (Frazer et al., 1997; Gonsamo et al., 2013; Hale and
86 Edwards, 2002; Rich, 1990). Both instruments incorporate an extreme wide angle view
87 to measure gap fraction – defined as the proportion of unobstructed sky in a given region
88 of the projected image plane (Frazer et al., 1997) – at multiple zenith angles. For
89 estimating understorey light levels, particularly during spring, wide viewing angles are an
90 advantage as sunlight largely penetrates the canopy below the zenith. Using gap fraction
91 measurements, Leaf Area Index (LAI) and canopy openness can be determined.

92 LAI is the most widely used metric of canopy structure (Jonckheere et al., 2005; Weiss et
93 al., 2004), though it is also one of the most difficult to characterise accurately (Bréda,
94 2003). LAI is defined as one half the total green leaf area per unit ground surface area
95 (Chen and Black, 1992). Hemispherical photography and PCAs assess the whole canopy
96 as viewed from a single point, using gap fraction inversion principles and radiative transfer
97 theory respectively (Chen et al., 1997; Macfarlane et al., 2007; Woodgate et al., 2015).
98 As such, LAI derived from optical methods actually characterises ‘Plant Area Index’ (as
99 trunks and branches are included as well as leaves), and is highly related to understorey
100 light levels (Bréda, 2003; Jonckheere et al., 2004). However, both methods are costly,
101 particularly PCAs, which in addition to high instrument costs, require simultaneous
102 reference light readings outside the canopy. This is problematic in forests, as a wireless
103 set up or remote data loggers are needed, adding additional resource implications and
104 making the method impractical for large-scale use (Bréda, 2003). Furthermore, both
105 methods for estimating LAI assume that canopy elements are randomly distributed. In
106 reality, a degree of ‘clumping’ occurs both within and between plant canopies (Bréda,
107 2003; Chen et al., 1997; Ryu et al., 2010; Weiss et al., 2004). The degree of clumping

108 varies depending on forest type and structure, and also shows strong seasonal variation
109 according to the phenological stage (Ryu et al., 2010). Therefore accurate LAI estimation
110 requires determination of a clumping index for a given canopy at a given time of year, and
111 specialist equipment and/or software is required (Chianucci et al., 2015; Ryu et al., 2010).

112 Digital Cover Photography (DCP) using ordinary digital cameras can also be used to
113 estimate LAI following the method proposed by Macfarlane et al. (2007). This method has
114 a number of advantages as specialist equipment and software are not required, though a
115 number of steps are involved in analysis to calculate effects of foliage clumping
116 (Chianucci et al., 2014; Macfarlane et al., 2007). DCP has been successfully used to track
117 canopy development in phenological studies concerned with photosynthesis and gas
118 exchange (Ryu et al., 2012). However, the restricted viewing angle of DCP cover
119 photography is less appropriate for tracking the progress of canopy closure, where the
120 objective is to assess change in the relative timing of shading in the understorey. Although
121 LAI is highly related to understorey light (particularly where it is based on gap fraction at
122 multiple zenith angles) it is primarily used to quantify ecophysiological attributes of forest
123 canopies (photosynthetic and transpiration rates) to study climate-biosphere interactions
124 (Bréda, 2003; Chen et al., 1997; Jonckheere et al., 2004; Macfarlane et al., 2007;
125 Woodgate et al., 2015). Where the aim is to track changes in relative canopy closure to
126 determine temporal variability in understorey light, canopy openness is a more
127 appropriate and straightforward metric to use (Brusa and Bunker, 2014).

128 Canopy openness is the proportion of the entire sky hemisphere that is unobstructed by
129 vegetation when viewed from a single point (Jennings et al., 1999), and is highly
130 correlated with understorey light (Brusa and Bunker, 2014; Gonsamo et al., 2013;
131 Pellikka, 2001; Promis et al., 2012; Roxburgh and Kelly, 1995; Whitmore et al., 1993).
132 Hemispherical photography has been widely used to assess canopy openness,
133 representing the sum of all gap fraction values, weighted according to zenith angle, and
134 multiplied by 100 to give a percent visible sky value (Frazer et al., 1997). The advent of
135 digital cameras and their increasing availability has made hemispherical photography
136 more widely available for forest science (Brusa and Bunker, 2014; Frazer et al., 2001;
137 Hale and Edwards, 2002; Inoue et al., 2004). However, cost and resource implications
138 still preclude many forest managers from using it as a monitoring tool. While
139 hemispherical photography does not require reference light readings to be made,
140 images must be taken under specific weather conditions – on dry, still days, without

141 direct sunlight, normally early or late in the day, or on a day with uniform overcast skies
142 (Rich, 1990). This places considerable constraint on when data can be collected. Once
143 images have been obtained, analysis can be time-consuming and expensive. Though
144 free specialist software programmes now exist that provide comparable results to
145 professional software (Promis et al., 2011), expertise is still required. Overall, the
146 technique is prohibitively expensive, in terms of cost and time, for phenology studies
147 that require high levels of replication.

148 A variety of cost-effective, rapid assessment alternatives to hemispherical photography
149 have been used to assess canopy openness, including photography without a fisheye
150 lens (Pellikka, 2001), the canopy scope (Brown et al., 2000), and simple visual
151 estimations (Jennings et al., 1999). These methods differ in their view zenith angle;
152 therefore canopy openness in this context is defined as the proportion of unobstructed
153 sky within the total area viewed. While these methods are used to characterise coarse-
154 level variation in canopy openness, their ability to detect fine-scale changes in canopies
155 through time needs to be assessed. Another option has emerged in the last few years
156 with the rise of smartphones that have high resolution cameras. Inexpensive fisheye
157 lens attachments for smartphones have recently become available for less than US\$10.
158 Smartphone photography, if reliable, could provide an efficient means of collecting large
159 quantities of data on the timing of canopy closure using citizen science.

160 The use of citizen science has proven highly successful in other areas of phenological
161 research, including observational studies of plant bud-burst and leaf-out timing
162 (Collinson and Sparks, 2008; Jeong et al., 2013; Mayer, 2010). The widespread and
163 increasing ownership of smartphones means that many people now carry sophisticated
164 cameras, making them ideal citizen science tools. However, a considerable range of
165 makes and models exist. These vary in their camera specifications (e.g. resolution,
166 focussing capability and angle of view), which could affect canopy openness
167 estimations (Frazer et al., 2001; Inoue et al., 2004; Jennings et al., 1999). Therefore, for
168 this method to be practical for large-scale use, different makes and models of
169 smartphone need to give comparable estimations.

170 In this study, we compared canopy openness values (% visible sky) from hemispherical
171 photography, with estimates derived from visual estimation techniques and from
172 smartphone photography, with and without the use of a fisheye lens attachment. Data
173 were collected in winter, spring, summer and autumn, at fixed points across four

174 broadleaved woodlands in south-west England, to assess the extent that surrogate
175 methods can estimate variation in canopy openness. We then tested a basic means of
176 analysing hemispherical photos and smartphone fisheye photos to derive canopy
177 openness using non-specialist image analysis software. We did this by comparing
178 simple canopy openness values (% visible sky) derived from the free image-analysis
179 software, with weighted canopy openness values (% visible sky weighted as a function
180 of gap fraction zenith angle) from professional specialist software. Recognising that
181 different makes of smartphone camera might perform differently, we also compared
182 three popular smartphone cameras in a separate trial. The different phone cameras
183 were tested in broadleaved woodland under three levels of canopy density, and with
184 multiple camera operators, to test reproducibility under different canopy conditions and
185 with different users.

186 Our overall objectives were: a) to identify whether any of the proposed surrogate
187 methods provide reliable estimates of variation in canopy openness; b) to identify
188 whether non-specialist image analysis software can produce comparable estimates to
189 specialist software; c) to test whether different smartphone camera models and different
190 camera users yield similar canopy openness estimations. It is important to note that this
191 study was not concerned with identifying methods to closely represent absolute values,
192 since it has already been established that methods incorporating different view angles
193 tend to give different absolute estimates of canopy openness (Bunnell and Vales, 1990;
194 Cook et al., 1995). Our focus was to identify whether any of the alternative methods
195 could reliably identify relative differences in canopy openness to monitor canopy closure
196 timings, and promote data collection through large-scale citizen science.

197 **2. Methods**

198 **2.1. Comparison of methods against hemispherical photography**

199 Trials took place in 2014 at four woodlands in Devon, England. The suite of sites was
200 purposely chosen to represent a range of canopy/understorey light conditions, with
201 varying aspect, composition and structure (Table 1). Six fixed sample points or 'stations'
202 were randomly selected in each of the four woodlands. At each station, canopy
203 openness was estimated by a variety of methods in each season (related to leaf
204 phenology): winter (no canopy), spring (around 50% leaf-out), summer (full canopy) and

205 autumn (around 50% leaf-drop). All estimates were made concurrently for a woodland
206 within each season, and the four woodlands all estimated within a week of each other.

207 2.1.1. Hemispherical photography

208 Hemispherical photographs were taken in colour using a Nikon Coolpix 990 3.34 MP
209 camera with Nikon Fisheye Converter FC-E8 lens (Nikon Corporation, Tokyo, Japan).
210 The circular fisheye lens provides a 180° field of view in all directions. Images were
211 taken using the basic quality setting and stored in VGA-size, as canopy openness
212 estimates are not affected by resolution or size settings with this camera model (Inoue
213 et al., 2004).

214 Photos were taken without rain or direct sunlight entering the lens (Rich, 1989). The
215 camera was mounted on a tripod at 1.2 m above ground, and levelled using a circular
216 bubble level. Pictures were taken using the camera timer function to reduce movement
217 during image capture (Rich, 1989). Aperture and shutter settings were set to automatic,
218 and to minimise error from over-exposure (Brusa and Bunker, 2014; Hale and Edwards,
219 2002), exposure was checked using the histogram function in the camera playback
220 facility, following the method outlined by Beckschafer et al. (2013). Where over-
221 exposure was apparent, exposure settings were manually lowered to -2.0 EV, the
222 minimum limit on this camera.

223 Images were analysed in HemiView Canopy Analysis Software v.2.1 (Delta-T Devices,
224 Cambridge, UK). The Coolpix 900 lens settings in HemiView were selected to correct
225 for lens distortion (Hale and Edwards, 2002). Various options exist for classifying a
226 photograph into “sky” and “not sky” (binarization), using image analysis software
227 (Glatthorn and Beckschafer, 2014; Zhao and He, 2016). In HemiView, it is only possible
228 to use manual thresholding of black and white pixels, so we followed this method, which
229 has been widely used in other studies (Bertin et al., 2011; Capdevielle-Vargas et al.,
230 2015; Hale and Edwards, 2002; Machado and Reich, 1999; Zhang et al., 2005). Each
231 photograph was individually processed to obtain the best contrast between vegetation
232 and the background sky, by visual comparison with the original photograph (Rich,
233 1990). A decision was made, based on visual assessment during threshold setting,
234 whether each photo should be included in the analysis. If it was not possible to gain a
235 good contrast between sky and vegetation across the whole image, that photo was
236 excluded. Canopy openness—in HemiView, “% visible sky”—was then derived for each

237 image by the software. In HemiView this value represents a weighted canopy openness
238 score based on gap fraction zenith angles (Rich et al., 1999).

239 Following analysis in HemiView, photos were also analysed using ImageJ (Rueden,
240 2016). Photos were converted to 8-bit binary black (“not sky”) and white (“sky”) images
241 in ImageJ. Following the same procedure as we used for photos in HemiView, the
242 manual thresholding function in ImageJ was used to individually process each image
243 and obtain the best contrast between vegetation and background sky. This was done
244 with reference to the original photograph (Rich, 1990). Hemispherical photos consist of
245 a circular image inside a rectangular frame. As ImageJ is not designed specifically for
246 such images, it cannot automatically exclude the framing pixels as is possible in
247 HemiView. Therefore to calculate canopy openness (the proportion of pixels classified
248 as sky) excluding the frame, we first calculated the number of pixels in a reference
249 image containing only open sky. We then used the ‘batch measure function’ to calculate
250 white (sky) pixels for all images, and calculated the canopy openness as a proportion of
251 the circular hemispherical image, excluding the framing pixels.

252 2.1.2. Smartphone photography with fisheye lens

253 Photos were taken using a Sony Xperia L smartphone camera (Android Version 5.0)
254 with magnetic fisheye lens attachment (Skimn FE-12 180° fisheye lens). Images were
255 taken at 5 MP using a 16:9 aspect ratio – the camera’s default settings. Using these
256 settings, the fisheye lens gave a 125° x 75° field of view. The smartphone was held
257 level, with the wider view orientated east-to-west when taking photos of the canopy, to
258 ensure comparable images were obtained for each season. Photographs were taken in
259 manual mode, with exposure lowered to -2.0 EV, the minimum limit on the camera.
260 Images were stored as high quality JPEGs, between 2–3 MB in size.

261 Smartphone fisheye photos were analysed in HemiView and ImageJ and visible sky
262 values were calculated, following the same procedures outlined for hemispherical photo
263 analysis. Lens equation coefficients relating zenith angles and radial distance were
264 calculated from a calibration curve constructed from measurements taken from
265 reference photographs. The resulting lens correction function ($y = 1.2213x -$
266 $1.396x^2 + 1.0855x^3 - 0.2761x^4$) was used by HemiView to adjust the calculations to correct
267 for lens distortion.

268 2.1.3. Smartphone photography without a fisheye lens

269 Smartphone photos were also taken of the canopy without the fisheye lens attachment,
270 giving a 70° x 40° field of view. Photos were taken of the canopy directly overhead (with
271 the wider view orientated east-west), and of the canopy facing in three different
272 bearings from the station – at 60°, 180° and 300° (with the camera positioned in a
273 landscape orientation at a 45° angle from the horizontal). All photos were taken
274 using the same settings as the photos with fisheye lens attachment, and exposure
275 settings were manually adjusted as previously described. Photographs were then
276 analysed using ImageJ, following the same procedure for binarization, to derive a
277 canopy openness estimation based on % visible sky. Two sets of canopy openness
278 estimates were derived from these photos: one based solely on the overhead canopy
279 photo, and one calculated as an average from all four photographs to incorporate a
280 wider area of view.

281 2.1.4. Non-photographic methods

282 Canopy openness was estimated visually on a simple percentage scale. Two sets of
283 canopy openness estimates were derived, one based solely on an overhead estimation,
284 and another based on an average of four estimations: one directly overhead, and at
285 three different bearings from the station (60°, 180° and 300°) at a 45° angle from the
286 horizontal.

287 Brown et al. (2000) proposed a canopy scope to aid in the visual estimation of canopy
288 openness. The scope consists of a simple Perspex sheet with a grid of twenty-five dots,
289 spaced 3cm apart in a 5x5 array. A 20cm length of string is attached to the corner, and
290 ensures the scope is held at a constant distance from the eyes when making
291 estimations. Canopy openness was estimated by focussing the scope on the largest
292 canopy gap visible from the station, and counting the number of dots coinciding with
293 sky. This number was then multiplied by four to obtain a percentage estimate. Brown et
294 al. (2000) found a close correlation between largest gap canopy openness and total
295 canopy openness, but acknowledged that for woodlands with several similar sized
296 canopy gaps, the largest gap estimate may not give an accurate representation. Two
297 alternative estimates were made: one by pointing the canopy scope at the canopy
298 directly overhead; and another by taking the mean of four canopy scope estimates
299 (using the overhead estimate and estimates made from viewing the canopy at bearings
300 of 60°, 180° and 300° from north, at an approximately 45° angle from the horizontal).

301 2.1.5. Statistical analysis

302 We used linear regression to compare canopy openness derived from hemispherical
303 photographs in HemiView, against each surrogate method. We first compared data from
304 all seasons and sites together to assess which methods were able to estimate broad
305 changes in canopy openness. We then compared methods on a season-by-season
306 basis across the four sites, to understand whether methods were capable of estimating
307 finer-scale variation in canopy openness. We also conducted method comparisons on a
308 site-by-site basis using data from all four seasons, to assess whether methods
309 performed well across the different woodlands.

310 For methods that performed consistently well across the comparisons, Analysis of
311 Covariance (ANCOVA) was used to test whether the methods estimated canopy
312 openness in similar ways under different conditions, with seasons and sites as
313 covariates. A Tukey-Kramer test was used to explore differences that were found
314 between seasons or sites. All statistical analyses were carried out in R 3.3 (R Core
315 Team, 2016).

316 **2.2. Comparison of smartphone models and operators**

317 2.2.1. Field imagery

318 A second trial comparing smartphone models and phone users took place in mixed
319 deciduous woodland at Mount Edgcumbe Estate, Cornwall (approximately 50°35'N and
320 4°16'W), during summer when trees were in full leaf. Three sampling locations or
321 'stations' were selected at the site, using visual assessment, to represent a 'closed',
322 'intermediate' and 'open' overhead canopy. We tested two popular Smartphone
323 cameras – the iPhone 5 and Samsung Galaxy S4 – against the Sony Xperia used in the
324 previous trials, to assess the comparability of canopy openness estimates. Photos taken
325 with the iPhone 5 had a resolution of 8 MP and an aspect ratio of 16:9, providing a 61° x
326 48° field of view. Photos taken with the Samsung Galaxy S4 had a resolution of 9.6 MP
327 and aspect ratio of 16:9, providing a 57° x 34° field of view. Photos were stored as high
328 quality JPEGS, between 2–3 MB in size.

329 Twenty-two volunteers consecutively took an overhead photograph of the canopy with
330 each camera, at each of the three stations. All photos were taken within a half-hour
331 period. Volunteers were instructed to hold the phone at an estimated level position and
332 take a photo of the canopy above, but were not told to orientate the phone in a

333 particular direction, as we were interested to see the extent that individual user
334 operation affected consistency in the results. Photos were analysed in ImageJ following
335 the procedure outlined above.

336 **2.2.2. Statistical analysis**

337 The Aligned Rank Transform (ART) procedure in the R package ARTTool (Kay and
338 Wobbrock, 2016), followed by separate ANOVA using R 3.3 (R Core Team, 2016), was
339 used to assess the effects of phone user, phone model and canopy treatment on
340 canopy openness values. The ART procedure is an appropriate way to analyse
341 datasets which are not normally distributed, and is described in more detail by
342 Wobbrock et al. (2011). We performed *post hoc* contrasts using estimated marginal
343 means with the emmeans package (Lenth, 2017).

344 **3. Results**

345 **3.1. Hemispherical photography with HemiView v other methods**

346 All hemispherical photos taken were suitably exposed in relation to sky conditions, for
347 inclusion in the analysis, while four smartphone fisheye photos and six smartphone
348 photos without the fisheye lens attachment were eliminated due to overexposure, out of
349 96 photos in each case.

350 Analysis of hemispherical photography with ImageJ produced reliable estimates of
351 canopy openness values derived from analysis with HemiView (Table 2, Figs 1A and
352 1D). With photos from spring, summer and autumn combined into a single ANCOVA
353 analysis, the slope of the relationship was no different for all three seasons (Fig. 1D
354 ANCOVA $F_{2,66} = 2.55, p = 0.09$). However, the intercepts of the relationships were
355 significantly different (Fig. 1D ANCOVA $F_{2,68} = 8.09, p < 0.001$), with summer values
356 estimated relatively lower than those of spring and autumn (Tukey-Kramer Test,
357 summer v spring $p = 0.004$, summer v autumn $p < 0.001$, spring v autumn $p = 0.864$).

358 None of the other methods closely estimated absolute canopy openness values derived
359 from hemispherical photography, but all smartphone photographic methods reliably
360 estimated relative differences in canopy openness across all seasons for all sites (Table
361 2, Figs 1B and 1C). The slopes of these relationships, which were all >1 , indicate that
362 smartphone fisheye photography results in higher estimates of canopy openness than
363 hemispherical photography, and that the estimates differ more at higher values of

364 canopy openness. During winter, when there were very high levels of canopy openness
365 ($mean = 37\%$, $sd = 5\%$), smartphone fisheye photos did not correspond reliably to
366 hemispherical photography (Table 2). This was also true for all other methods tested,
367 and since winter is not a season where canopy change is expected and therefore not
368 relevant to our aims, winter data were excluded from the rest of the analyses. Non-
369 photographic methods (canopy scope and simple visual estimations) were much poorer
370 estimators of change in canopy openness across all seasons and sites (Table 2).

371 Smartphone with fisheye lens estimates taken in different seasons had similar slope
372 relationships (Fig. 1E ANCOVA $F_{2,66} = 0.31$, $p = 0.73$; Fig. 1F $F_{2,66} = 0.64$, $p = 0.53$), but
373 they varied in intercept (Fig 1E, ANCOVA $F_{2,64} = 33.56$, $p < 0.001$; Fig. 1F $F_{2,64} = 48.73$,
374 $p < 0.001$). For smartphone photographs analysed with HemiView canopy analysis
375 software, spring and autumn intercepts were not significantly different (Tukey-Kramer p
376 = 0.796), but both were significantly different from summer ($p < 0.001$ in each case).
377 The same photographs analysed with ImageJ had different intercepts for each of the
378 three seasons (spring v autumn $p = 0.020$, spring v summer $p < 0.001$, summer v
379 autumn $p < 0.001$).

380 Since smartphone fisheye photography and ImageJ analysis reliably estimated variation
381 in canopy openness, we tested whether the methods performed consistently between
382 different sites (Fig. 2). Hemispherical imagery analysed with ImageJ showed similar
383 slope relationships across all sites (Fig. 2A; ANCOVA $F_{3,64} = 1.17$, $p = 0.33$), but
384 significant differences in intercept (ANCOVA $F_{3,67} = 4.75$, $p = 0.005$). The intercept of
385 Hardwick was different from Hunshaw and Whitleigh (Tukey-Kramer Test, $p = 0.018$
386 and $p = 0.007$), though all other intercepts were not different ($p = 0.288$ to 1.000).

387 Smartphone with fisheye photography, whether analysed with HemiView or ImageJ,
388 resulted in different slope relationships for Hardwick compared to the other sites (Fig.
389 2B, ANCOVA $F_{3,60} = 4.10$, $p = 0.010$; Fig. 2C, $F_{3,60} = 7.07$, $p < 0.001$). As canopy
390 openness increased, the estimates for Hardwick differed less from the hemispherical
391 standard than the other sites. The intercepts of the other sites did not differ (Fig. 2B,
392 ANCOVA $F_{2,46} = 0.91$, $p = 0.41$; Fig. 2C, $F_{2,46} = 0.54$, $p = 0.59$).

393 3.2. Comparison of smartphone models and operators

394 The three canopy treatments (closed, intermediate and open) were clearly different from
395 each other in terms of canopy openness, but it did not matter which phone model or

396 user took the photos (Fig. 3; Aligned Rank Transform + ANOVA, $p_{\text{canopy}} < 0.0001$, p_{user}
397 = 1.00 and $p_{\text{model}} = 0.50$). However, variability in estimation of canopy openness
398 increased markedly as canopy openness increased. For the closed canopy, standard
399 deviations of the estimates ranged from 0.79–1.46% canopy openness, but were much
400 greater for the open canopy (7.42–12.43%).

401 **4. Discussion**

402 Our results showed that smartphone photographic methods estimated variation in
403 canopy closure effectively, but rapid visual estimation methods did not. Basic visual
404 estimations of canopies are known to lack consistency, varying considerably due to
405 weather conditions (Jennings et al., 1999) and observer biases (Vales and Bunnell,
406 1988). The canopy scope is more a quantitative visual estimation method, allowing for
407 greater consistency and has been shown to have low between-observer bias (Brown et
408 al., 2000), so is potentially more suitable for citizen science. However, while the canopy
409 scope can distinguish quite different degrees of canopy openness (Brown et al., 2000),
410 it lacked the fine resolution needed to distinguish between similar canopies, and
411 therefore is less suitable for monitoring changes through time.

412 Smartphone photographic methods have now become a cost effective and practical
413 alternative to visual estimation. Simple photographs using a smartphone camera without
414 a lens attachment were sufficient for assessing the degree of variation in canopies
415 across a whole season, but did not pick up fine-scale variations (i.e. between similar
416 canopies within a season) compared with hemispherical photography. This is
417 unsurprising, as their narrow angle of view means they are essentially providing an
418 estimate of canopy cover directly overhead, as opposed to canopy closure across a
419 range of zenith angles (Chianucci et al., 2014; Jennings et al., 1999). With the addition
420 of an inexpensive fisheye lens attachment, smartphone photographs were able to pick
421 up finer variations in canopy openness in spring, summer and autumn, which would be
422 important for monitoring seasonal dynamics.

423 As anticipated, smartphone fisheye photography gave higher canopy openness
424 estimations than hemispherical photography, due to its narrower field of view. With
425 hemispherical photography, an image taken within a forest will typically include a ring of
426 tree trunks and shrubs around the periphery, with low gap fractions in the outer portions
427 of the image (at larger zenith angles) (Chen et al., 1997). Although incorporating a

428 greater field of view than non-fisheye photos, smartphone fisheye photos still omit the
429 largest zenith angles containing most of the lower trunks and shrub layer. In its field of
430 view, the gaps in a canopy contribute more to the overall image. Similarly, twigs and
431 foliage have higher prominence in images. As smartphone fisheye photography misses
432 gaps at larger zenith angles, it would not be a suitable method for detailed studies of
433 canopy structure or plant growth. However, the method is suitable for monitoring timing
434 of canopy closure, and its narrower field of view could actually make it a superior
435 method for identifying leafing activity early in spring.

436 We found canopy structure affected the relationship between hemispherical
437 photography and smartphone photography, meaning that canopy openness values must
438 be converted to proportions of total canopy closure to be correctly interpreted. Where
439 the overhead canopy was uniformly closed, the difference between canopy openness
440 estimations from smartphone fisheye photos and hemispherical photos was lower –
441 both sets of images show a closed canopy with few gaps. In more open situations, the
442 difference between the two sets of estimations was greater. Similarly where stand
443 density was higher and the height of the tree canopy was lower (e.g. at Hardwick Wood,
444 Table 1), the difference between canopy openness values from the two methods was
445 smaller. Canopy height is known to effect openness estimations when the field of view
446 is reduced (Jennings et al., 1999; Pellikka, 2001).

447 Due to the influence of canopy structure on canopy openness values, we propose this
448 method is appropriate for monitoring relative change in canopies through time. In order
449 to compare the timing and rate of canopy closure across different forest locations we
450 can standardize along a proportional scale of canopy closure, where 0% represents the
451 winter canopy value prior to budburst, and 100% represents the summer canopy value
452 once the canopy is fully in leaf. We note that canopies are dynamic, and small-scale
453 fluctuations occur through summer. Therefore the summer canopy value would be
454 determined from the point where the canopy reaches ‘adjustment stability’ (Margalef,
455 1969), after which only small changes of less than 2% canopy closure are observed.
456 The progress of canopy closure can then be plotted through time from 0–100%, and a
457 logistic growth model can be fitted to characterise the phenological pattern (Richardson
458 et al., 2006; Zhang et al., 2003). An example using smartphone fish-eye photography is
459 provided in Supplementary Material.

460 In terms of photo analysis, we found that ImageJ is a reasonable alternative to
461 professional specialist software such as HemiView, for deriving relative canopy
462 openness values. It is clear that ImageJ overestimates values from HemiView to some
463 degree, so again, this method would not be suitable for studies where absolute values
464 were needed. The distortion of a hemispherical or fisheye lens causes the central part
465 of the image, towards the zenith, to appear larger than peripheral elements towards the
466 horizon (Herbert, 1987). Canopy openness derived from HemiView is based on a
467 weighted gap fraction that takes into account the zenith angle of canopy gaps, and
468 corrects for a given lens distortion (Promis et al., 2011). In contrast, canopy openness
469 derived from ImageJ is simply the percentage visible sky across the image. However,
470 values from ImageJ still consistently and reliably estimated relative differences in
471 canopy openness in our study.

472 ImageJ has the benefits of being free, open access and relatively straightforward to use.
473 It is not necessary to provide specifications of the fisheye lens to use it. Image
474 binarization is still required, which can be time consuming. The manual thresholding
475 technique used in this study would not be suitable for analysing large quantities of
476 citizen science data. Many citizen science projects have successfully utilised internet
477 crowd-sourcing applications (Kosmala et al., 2016) to involve the public in processing
478 and classifying large numbers of images, so a similar approach could be used to
479 binarize canopy photos, with multiple people classifying pixels for the same image to
480 reduce error (Inoue et al., 2011). However, new methods for automatic thresholding of
481 photos would improve efficiency (Brusa and Bunker, 2014; Glatthorn and Beckschafer,
482 2014; Inoue et al., 2004), and auto-thresholding plug-ins for ImageJ (Glatthorn and
483 Beckschafer, 2014) could provide a viable option.

484 In terms of practicalities, smartphone fisheye photography is suitable for widespread
485 use as part of citizen science projects, and if managed properly is a game-changer in
486 terms of data quantity. The good agreement between smartphone models and users
487 suggests the method can be reliably applied by citizen scientists. The three phone
488 models tested varied in resolution and field of view, but still produced comparable
489 results. While some variation was evident between photos taken with the same phone,
490 under the same canopy conditions, there was no overall effect of phone user on canopy
491 openness values. Variation between photos taken with the same phone was greatest at
492 higher levels of canopy openness. This is not surprising, as under the dense canopy,

493 gaps were small and uniformly distributed, whereas the open canopy comprised a very
494 large central gap bordered by canopy. Small variation in camera positioning could
495 therefore result in compositional differences between photographs. This could lead to
496 significant differences in estimates, as has been observed with other methods for
497 estimating canopy openness (Jennings et al. 1999). Therefore, we recommend that for
498 best results camera position is standardised by installation of fixed camera mounts
499 (University of New Hampshire, 2017) for citizen scientists to place their smartphones on
500 in order to take repeat photographs of particular parts of the canopy.

501 The quality of photos obtained from smartphone fisheye photography is sufficient to
502 obtain reliable data. The high resolution available with smartphone cameras is a clear
503 advantage. Resolution is known to be an important factor influencing the quality of
504 canopy openness measures from hemispherical photography (Brusa and Bunker, 2014;
505 Woodgate et al., 2015), and in this study the smartphone camera resolution was
506 superior to that of the hemispherical camera (with nearly 2,000,000 more pixels). It has
507 also been noted that higher resolution images are less vulnerable to thresholding errors
508 during image processing and analysis (Macfarlane et al., 2007). Some blurring was
509 evident towards the perimeter of the smartphone fisheye photos, but this is also
510 apparent with hemispherical photos (Frazer et al., 2001). Blurring from motion caused
511 by holding the camera to capture images could also influence image quality (Woodgate
512 et al., 2015). The use of fixed mounts for phone cameras would help alleviate this
513 problem, as well as utilising the camera's timer function or earphone controls to
514 remotely operate the camera shutter.

515 As with hemispherical photography, there are several logistical issues associated with
516 the use of smartphone photography, relating to sky conditions and image exposure. The
517 effects of over-exposure and the importance of taking photos under uniform sky
518 conditions has been emphasised in many studies (Beckschafer et al., 2013; Brusa and
519 Bunker, 2014; Rich, 1990; Woodgate et al., 2015; Zhang et al., 2005). In this study, a
520 small proportion of smartphone photos had to be excluded due to over-exposure. While
521 smartphone photographs were taken at -2.0 EV, the lowest exposure setting available,
522 Beckschafer et al. (2013) showed that over-exposure can still occur at -2.0 EV under
523 bright skies. This can also be a problem with hemispherical photography, as the Nikon
524 Coolpix 990 had the same limits for exposure compensation. The histogram function
525 allows a definitive check as to whether photos are over-exposed, and more advanced

526 cameras allow for lowering below -2.0 EV (Beckschafer et al., 2013). We emphasise
527 again that the smartphone fish-eye photography method would not be suitable for
528 detailed studies of canopy structure or growth where small differences between sites
529 must be detected, and therefore consistent exposure is paramount (Leblanc, 2005).
530 However, to track the progress of canopy closure through time and compare trends in
531 the timing of this phenological event over large spatial scales, a small degree of noise in
532 the data is acceptable. The example in Supplementary Material demonstrates that the
533 phenological process of canopy closure can be clearly modelled using this method.
534 While the limits of exposure settings on smartphone cameras may mean some photos
535 have to be discarded, the greater number of images obtained by utilising a citizen
536 science approach should increase the number of suitable images that can be included
537 in a study. Where possible citizen scientists should be encouraged to take photos early
538 or late in the day, which is when sky conditions are generally most appropriate, and
539 coincides with times when people are likely to be available to collect imagery.

540 **5. Conclusions**

541 Smartphone fisheye photography, with relatively simple image analysis, offers a
542 practical method for comparing changes in the timing of canopy closure across different
543 forests year on year, and may even be more suited to this task than hemispherical
544 photography. Using this approach, trends in proportional changes in canopy closure
545 could be identified across different spatial and temporal scales using citizen science.
546 Further research is required to assess the temporal resolution of image capture needed
547 to represent canopy changes adequately.

548 **6. Acknowledgements**

549 We would like to thank Jacqueline and Adrian Wolfe, Clinton Devon Estates, and the
550 Woodland Trust for granting permission to study their woodlands. Nicola Steer helped
551 with the modelling of our datasets in Supplementary Material. Conservation Biology
552 students at University of Plymouth participated in the smartphone photo trials: Eleanor
553 Arthur, Mike Cox, Megan Dalton, Emily Daniel, Jacob Dansie, John Davey, Rebecca
554 Dickson, Simon Harrington, Ziad Ibbini, Alex King, Niall Legg, Jordan Maskell, Ella
555 Mutch, Guy Palmer, Scott Patterson, Julian Prow, James Robertshaw, Jessica
556 Robertson, Emma Shadbolt, Rhys Smith, Jack Whittington and Jamie Witherford. This

557 research did not receive a grant from funding agencies in the public, commercial, or not-
 558 for-profit sectors.

559 **7. References**

- 560 Augspurger, C.K., 2008. Early spring leaf out enhances growth and survival of saplings in a
 561 temperate deciduous forest. *Oecologia*, 156(2): 281-286.
- 562 Beckschafer, P., Seidel, D., Kleinn, C. and Xu, J.C., 2013. On the exposure of hemispherical
 563 photographs in forests. *J. Biogeosci. For.*, 6(4): 228-237.
- 564 Bertin, S., Palmroth, S., Kim, H.S., Perks, M.P., Mencuccini, M. and Oren, R., 2011. Modelling
 565 understorey light for seedling regeneration in continuous cover forestry canopies.
 566 *Forestry*, 84(4): 397-409.
- 567 Boyd, D.S., Almond, S., Dash, J., Curran, P.J. and Hill, R.A., 2011. Phenology of vegetation in
 568 Southern England from Envisat MERIS terrestrial chlorophyll index (MTCI) data. *Int. J.*
 569 *Remote Sens.*, 32(23): 8421-8447.
- 570 Bréda, N.J.J., 2003. Ground-based measurements of leaf area index: a review of methods,
 571 instruments and current controversies. *J. Exp. Bot.*, 54(392): 2403-2417.
- 572 Brown, N., Jennings, S., Wheeler, P. and Nabe-Nielsen, J., 2000. An improved method for the
 573 rapid assessment of forest understorey light environments. *J. Appl. Ecol.*, 37(6): 1044-
 574 1053.
- 575 Brusa, A. and Bunker, D.E., 2014. Increasing the precision of canopy closure estimates from
 576 hemispherical photography: Blue channel analysis and under-exposure. *Agric. For.*
 577 *Meteorol.*, 195-196: 102-107.
- 578 Bunnell, F.L. and Vales, D.J., 1990. Comparison of methods for estimating forest overstory
 579 cover: differences among techniques. *Can. J. Forest Res.*, 20(1): 101-107.
- 580 Capdevielle-Vargas, R., Estrella, N. and Menzel, A., 2015. Multiple-year assessment of
 581 phenological plasticity within a beech (*Fagus sylvatica* L.) stand in southern Germany.
 582 *Agric. For. Meteorol.*, 211-212: 13-22.
- 583 Chen, J.M. and Black, T.A., 1992. Defining leaf-area index for non-flat leaves. *Plant Cell Environ.*,
 584 15(4): 421-429.
- 585 Chen, J.M., Rich, P.M., Gower, S.T., Norman, J.M. and Plummer, S., 1997. Leaf area index of
 586 boreal forests: Theory, techniques, and measurements. *J. Geophys. Res. Atmos.*,
 587 102(D24): 29429-29443.
- 588 Chianucci, F., Chiavetta, U. and Cutini, A., 2014. The estimation of canopy attributes from digital
 589 cover photography by two different image analysis methods. *iForest Biogeosci. For.*, 7:
 590 255-259.
- 591 Chianucci, F., Macfarlane, C., Pisek, J., Cutini, A. and Casa, R., 2015. Estimation of foliage
 592 clumping from the LAI-2000 Plant Canopy Analyzer: effect of view caps. *Trees-Struct.*
 593 *Funct.*, 29(2): 355-366.
- 594 Cleland, E.E., Chuine, I., Menzel, A., Mooney, H.A. and Schwartz, M.D., 2007. Shifting plant
 595 phenology in response to global change. *Trends Ecol. Evol.*, 22(7): 357-365.

- 596 Collinson, N. and Sparks, T., 2008. Phenology—Nature's Calendar: an overview of results from
597 the UK Phenology Network. *Arboric. J.*, 30(4): 271-278.
- 598 Cook, J.G., Stutzman, T.W., Bowers, C.W., Brenner, K.A. and Irwin, L.L., 1995. Spherical
599 densiometers produce biased estimators of forest canopy cover. *Wildlife Soc. B.*, 23:
600 711–717.
- 601 De Frenne, P., Brunet, J., Shevtsova, A., Kolb, A., Graae, B.J., Chabrerie, O., Cousins, S.A.O.,
602 Decocq, G., De Schrijver, A., Diekmann, M., Gruwez, R., Heinken, T., Hermy, M., Nilsson,
603 C., Stanton, S., Tack, W., Willaert, J. and Verheyen, K., 2011. Temperature effects on
604 forest herbs assessed by warming and transplant experiments along a latitudinal
605 gradient. *Global Change Biol.*, 17(10): 3240-3253.
- 606 Engelbrecht, B.M.J. and Herz, H.M., 2001. Evaluation of different methods to estimate
607 understorey light conditions in tropical forests. *J. Trop. Ecology*, 17(2): 207-224.
- 608 Engelhardt, M.J. and Anderson, R.C., 2011. Phenological niche separation from native species
609 increases reproductive success of an invasive species: *Alliaria petiolata* (Brassicaceae) -
610 garlic mustard. *J. Torrey Bot. Soc.*, 138(4): 418-433.
- 611 Fisher, J.I., Mustard, J.F. and Vadeboncoeur, M.A., 2006. Green leaf phenology at Landsat
612 resolution: Scaling from the field to the satellite. *Remote Sens. Environ.*, 100(2): 265-
613 279.
- 614 Frazer, G.W., Fournier, R.A., Trofymow, J.A. and Hall, R.J., 2001. A comparison of digital and film
615 fisheye photography for analysis of forest canopy structure and gap light transmission.
616 *Agric. For. Meteorol.*, 109(4): 249-263.
- 617 Frazer, G.W., Trofymow, J.A. and Lertzman, K.P., 1997. A method for estimating canopy
618 openness, effective leaf area index, and photosynthetically active photon flux density
619 using hemispherical photography and computerized image analysis techniques. *Nat.*
620 *Res. Canada, Can. For. Serv. Pacific For. Cent. Inf. Re BC-X-373*, pp 75.
- 621 Gendron, F., Messier, C. and Comeau, P.G., 1998. Comparison of various methods for
622 estimating the mean growing season percent photosynthetic photon flux density in
623 forests. *Agric. For. Meteorol.*, 92(1): 55-70.
- 624 Giasson, M.A., Ellison, A.M., Bowden, R.D., Crill, P.M., Davidson, E.A., Drake, J.E., Frey, S.D.,
625 Hadley, J.L., Lavine, M., Melillo, J.M., Munger, J.W., Nadelhoffer, K.J., Nicoll, L., Ollinger,
626 S.V., Savage, K.E., Steudler, P.A., Tang, J., Varner, R.K., Wofsy, S.C., Foster, D.R. and Finzi,
627 A.C., 2013. Soil respiration in a northeastern US temperate forest: a 22-year synthesis.
628 *Ecosphere*, 4(11): 1-28.
- 629 Glatthorn, J. and Beckschafer, P., 2014. Standardizing the protocol for hemispherical
630 photographs: accuracy assessment of binarization algorithms. *PLoS One*, 9(11).
- 631 Gonsamo, A., D'Odorico, P. and Pellikka, P., 2013. Measuring fractional forest canopy element
632 cover and openness - definitions and methodologies revisited. *Oikos*, 122(9): 1283-1291.
- 633 Hale, S.E. and Edwards, C., 2002. Comparison of film and digital hemispherical photography
634 across a wide range of canopy densities. *Agric. For. Meteorol.*, 112(1): 51-56.
- 635 Hamunyela, E., Verbesselt, J., Roerink, G. and Herold, M., 2013. Trends in Spring Phenology of
636 Western European Deciduous Forests. *Remote Sens.*, 5(12): 6159.

- 637 Herbert, T.J., 1987. Area projections of fisheye photographic lenses. Agric. For. Meteorol., 39(2-
638 3): 215-223.
- 639 Inoue, A., Yamamoto, K. and Mizoue, N., 2011. Comparison of automatic and interactive
640 thresholding of hemispherical photography. J. For. Sci., 57: 78-87.
- 641 Inoue, A., Yamamoto, K., Mizoue, N. and Kawahara, Y., 2004. Effects of image quality, size and
642 camera type on forest light environment estimates using digital hemispherical
643 photography. Agric. For. Meteorol., 126(1-2): 89-97.
- 644 Jennings, S.B., Brown, N.D. and Sheil, D., 1999. Assessing forest canopies and understorey
645 illumination: canopy closure, canopy cover and other measures. Forestry, 72(1): 59-73.
- 646 Jeong, S., Medvigy, D., Shevliakova, E. and Malyshev, S., 2013. Predicting changes in temperate
647 forest budburst using continental-scale observations and models. Geophys. Res. Lett.,
648 40(2): 359-364.
- 649 Jonckheere, I., Fleck, S., Nackaerts, K., Muys, B., Coppin, P., Weiss, M. and Baret, F., 2004.
650 Review of methods for in situ leaf area index determination - Part I. Theories, sensors
651 and hemispherical photography. Agric. For. Meteorol., 121(1-2): 19-35.
- 652 Jonckheere, I., Nackaerts, K., Muys, B. and Coppin, P., 2005. Assessment of automatic gap
653 fraction estimation of forests from digital hemispherical photography. Agric. For.
654 Meteorol., 132(1): 96-114.
- 655 Kay, M. and Wobbrock, J.O., 2016. ARTTool: Aligned Rank Transform for Nonparametric Factorial
656 ANOVAs. R package version 0.10.4, <https://github.com/mjskay/ARTTool>.
- 657 Kim, H.J., Jung, J.B., Jang, Y.L., Sung, J.H. and Park, P.S., 2015. Effects of experimental early
658 canopy closure on the growth and reproduction of spring ephemeral *Erythronium*
659 *japonicum* in a montane deciduous forest. J. Plant Biol., 58(3): 164-174.
- 660 Kosmala, M., Crall, A., Cheng, R., Hufkens, K., Henderson, S. and Richardson, A.D., 2016. Season
661 Spotter: Using Citizen Science to Validate and Scale Plant Phenology from Near-Surface
662 Remote Sensing. Remote Sens., 8(9).
- 663 Leblanc, S.G., 2005. Digital Hemispherical Photography Manual (v. 1.2). Natural Resources
664 Canada - Canada Centre for Remote Sensing, Saint-Hubert, Québec, 28 pp.
- 665 Lenth, R., 2017. emmeans: Estimated Marginal Means, aka Least-Squares Means. R package
666 version 1.0, <https://CRAN.R-project.org/package=emmeans>.
- 667 Macfarlane, C., Hoffman, M., Eamus, D., Kerp, N., Higginson, S., McMurtrie, R. and Adams, M.,
668 2007. Estimation of leaf area index in eucalypt forest using digital photography. Agric.
669 For. Meteorol., 143(3): 176-188.
- 670 Machado, J.L. and Reich, P.B., 1999. Evaluation of several measures of canopy openness as
671 predictors of photosynthetic photon flux density in deeply shaded conifer-dominated
672 forest understory. Can. J. Forest Res., 29(9): 1438-1444.
- 673 Margalef, R., 1969. Diversity and stability: A practical proposal and a model of
674 interdependence. In: G.M. Woodwell and H.H. Smith (Editors), Diversity and Stability in
675 Ecological Systems, Brookhaven Symposium in Biology, No 22. Brookhaven National
676 Laboratory, New York, pp. 25-37.
- 677 Mayer, A., 2010. Phenology and citizen science. Bioscience, 60(3): 172-175.

- 678 Menzel, A. and Fabian, P., 1999. Growing season extended in Europe. *Nature*, 397(6721): 659-
679 659.
- 680 Menzel, A., Sparks, T.H., Estrella, N., Koch, E., Aasa, A., Ahas, R., Alm-Kubler, K., Bissolli, P.,
681 Braslavka, O., Briede, A., Chmielewski, F.M., Crepinsek, Z., Curnel, Y., Dahl, A., Defila, C.,
682 Donnelly, A., Filella, Y., Jatcza, K., Mage, F., Mestre, A., Nordli, O., Penuelas, J., Pirinen,
683 P., Remisova, V., Scheifinger, H., Striz, M., Susnik, A., Van Vliet, A.J.H., Wielgolaski, F.E.,
684 Zach, S. and Zust, A., 2006. European phenological response to climate change matches
685 the warming pattern. *Global Change Biol.*, 12(10): 1969-1976.
- 686 Pellikka, P., 2001. Application of vertical skyward wide-angle photography and airborne video
687 data for phenological studies of beech forests in the German Alps. *Int. J. Remote Sens.*,
688 22(14): 2675-2700.
- 689 Promis, A., Caldentey, J. and Cruz, G., 2012. Evaluating the usefulness of hemispherical
690 photographs as a means to estimate photosynthetic photon flux density during a
691 growing season in the understorey of *Nothofagus pumilio* forests. *Plant Biosyst.*, 146(1):
692 237-243.
- 693 Promis, A., Gärtner, S.M., Butler-Manning, D., Durán-Rangel, C., Rief, A., Cruz, G. and
694 Hernández, L., 2011. Comparison of four different programs for the analysis of
695 hemispherical photographs using parameters of canopy structure and solar radiation
696 transmittance. *Waldökologie*, 11: 19-33.
- 697 R Core Team, 2016. R: A language and environment for statistical computing. R Foundation for
698 Statistical Computing, Vienna, Austria
- 699 Rich, P.M., 1989. A manual for analysis of hemispherical canopy photography. Technical Report,
700 Los Alamos National Lab., NM, USA.
- 701 Rich, P.M., 1990. Characterizing plant canopies with hemispherical photographs. *Remote Sens.*
702 Rev., 5(1): 13-29.
- 703 Rich, P.M., Wood, J., Vieglais, D.A., Burek, K. and Webb, N., 1999. User manual for HemiView
704 version 2.1. Delta-T Devices, United Kingdom.
- 705 Richardson, A.D., Bailey, A.S., Denny, E.G., Martin, C.W. and O'Keefe, J., 2006. Phenology of a
706 northern hardwood forest canopy. *Global Change Biol.*, 12(7): 1174-1188.
- 707 Richardson, A.D., Keenan, T.F., Migliavacca, M., Ryu, Y., Sonnentag, O. and Toomey, M., 2013.
708 Climate change, phenology, and phenological control of vegetation feedbacks to the
709 climate system. *Agric. For. Meteorol.*, 169: 156-173.
- 710 Roberts, A.M.I., Tansey, C., Smithers, R.J. and Phillimore, A.B., 2015. Predicting a change in the
711 order of spring phenology in temperate forests. *Global Change Biol.*, 21(7): 2603-2611.
- 712 Roxburgh, J.R. and Kelly, D., 1995. Uses and limitations of hemispherical photography for
713 estimating forest light environments. *N. Z. J. Ecol.*, 19(2): 213-217.
- 714 Rueden, C., Dietz, C., Horn, M., Schindelin, J., Northan, B., Berthold, M., Eliceiri, K. , 2016.
715 ImageJ Ops [Software]. <http://imagej.net/Ops>.
- 716 Ryu, Y., Nilson, T., Kobayashi, H., Sonnentag, O., Law, B.E. and Baldocchi, D.D., 2010. On the
717 correct estimation of effective leaf area index: Does it reveal information on clumping
718 effects? *Agric. For. Meteorol.*, 150(3): 463-472.

- 719 Ryu, Y., Verfaillie, J., Macfarlane, C., Kobayashi, H., Sonnentag, O., Vargas, R., Ma, S. and
720 Baldocchi, D.D., 2012. Continuous observation of tree leaf area index at ecosystem scale
721 using upward-pointing digital cameras. *Remote Sens. Environ.*, 126: 116-125.
- 722 Thompson, R. and Clark, R.M., 2008. Is spring starting earlier? *Holocene*, 18(1): 95-104.
- 723 University of New Hampshire, 2017. Picture Post. <https://picturepost.unh.edu/index.jsp>
724 Accessed: December 18, 2017.
- 725 Vales, D.J. and Bunnell, F.L., 1988. Comparison of methods for estimating forest overstory
726 cover: differences among techniques. *Can. J. Forest Res.*, 20(1): 101-107.
- 727 Van Couwenberghe, R., Collet, C., Lacombe, E. and Gegout, J.C., 2011. Abundance response of
728 western European forest species along canopy openness and soil pH gradients. *For. Ecol.
729 Manage.*, 262(8): 1483-1490.
- 730 Vitasse, Y., Francois, C., Delpierre, N., Dufrêne, E., Kremer, A., Chuine, I. and Delzon, S., 2011.
731 Assessing the effects of climate change on the phenology of European temperate trees.
732 *Agric. For. Meteorol.*, 151(7): 969-980.
- 733 Wang, S., Yang, B., Yang, Q., Lu, L., Wang, X. and Peng, Y., 2016. Temporal Trends and Spatial
734 Variability of Vegetation Phenology over the Northern Hemisphere during 1982-2012.
735 *PLoS One*, 11(6): e0157134.
- 736 Weiss, M., Baret, F., Smith, G.J., Jonckheere, I. and Coppin, P., 2004. Review of methods for in
737 situ leaf area index (LAI) determination. *Agric. For. Meteorol.*, 121(1): 37-53.
- 738 White, K., Pontius, J. and Schaberg, P., 2014. Remote sensing of spring phenology in
739 northeastern forests: A comparison of methods, field metrics and sources of
740 uncertainty. *Remote Sens. of Environ.*, 148: 97-107.
- 741 White, M.A., De Beurs, K.M., Didan, K., Inouye, D.W., Richardson, A.D., Jensen, O.P., O'Keefe, J.,
742 Zhang, G., Nemani, R.R., Van Leeuwen, W.J.D., Brown, J.F., De Wit, A., Schaepman, M.,
743 Lin, X., Dettinger, M., Bailey, A.S., Kimball, J., Schwartz, M.D., Baldocchi, D.D., Lee, J.T.
744 and Lauenroth, W.K., 2009. Intercomparison, interpretation, and assessment of spring
745 phenology in North America estimated from remote sensing for 1982–2006. *Global
746 Change Biol.*, 15(10): 2335-2359.
- 747 Whitmore, T.C., Brown, N.D., Swaine, M.D., Kennedy, D., Goodwin-Bailey, C.I. and Gong, W.K.,
748 1993. Use of hemispherical photographs in forest ecology: measurement of gap size and
749 radiation totals in a Bornean tropical rain forest. *J. Trop. Ecology*, 9(2): 131-151.
- 750 Willis, C.G., Ruhfel, B.R., Primack, R.B., Miller-Rushing, A.J., Losos, J.B. and Davis, C.C., 2010.
751 Favorable climate change response explains non-native species' success in Thoreau's
752 Woods. *PLoS One*, 5(1).
- 753 Wobbrock, J.O., Findlater, L., Gergle, D. and Higgins, J.J., 2011. The Aligned Rank Transform for
754 nonparametric factorial analyses using only ANOVA procedures. , ACM Conference on
755 Human Factors in Computing Systems (CHI '11), Vancouver, British Columbia (May 7-12,
756 2011). ACM Press, New York, pp. 143-146.
- 757 Woodgate, W., Jones, S.D., Suarez, L., Hill, M.J., Armston, J.D., Wilkes, P., Soto-Berelov, M.,
758 Haywood, A. and Mellor, A., 2015. Understanding the variability in ground-based
759 methods for retrieving canopy openness, gap fraction, and leaf area index in diverse
760 forest systems. *Agric. For. Meteorol.*, 205: 83-95.

- 761 Wu, X. and Liu, H., 2013. Consistent shifts in spring vegetation green-up date across temperate
762 biomes in China, 1982–2006. *Global Change Biol.*, 19(3): 870-880.
- 763 Yuste, J.C., Janssens, I.A., Carrara, A. and Ceulemans, R., 2004. Annual Q(10) of soil respiration
764 reflects plant phenological patterns as well as temperature sensitivity. *Global Change
765 Biol.*, 10(2): 161-169.
- 766 Zhang, X., Friedl, M.A., Schaaf, C.B., Strahler, A.H., Hodges, J.C.F., Gao, F., Reed, B.C. and Huete,
767 A., 2003. Monitoring vegetation phenology using MODIS. *Remote Sens. Environ.*, 84(3):
768 471-475.
- 769 Zhang, Y.Q., Chen, J.M. and Miller, J.R., 2005. Determining digital hemispherical photograph
770 exposure for leaf area index estimation. *Agric. For. Meteorol.*, 133(1-4): 166-181.
- 771 Zhao, K.N. and He, F.L., 2016. Estimating light environment in forests with a new thresholding
772 method for hemispherical photography. *Can. J. Forest Res.*, 46(9): 1103-1110.
- 773

774 **Tables**

775

Site	Size (ha)	Stand density (trees/ha)	Average tree height (m)	Aspect	Dominant canopy species	Dominant shrub layer species
Hardwick Wood (50°22'N, 4°4'W)	22	1360	16	Flat	<i>Acer pseudoplatanus</i> , <i>Fraxinus excelsior</i>	<i>Acer pseudeoplatus</i> , <i>Ulmus</i> sp.
Hunshaw Wood (50°55'N, 4°7'W)	18	556	30	S	<i>Quercus robur</i> with <i>Fagus sylvatica</i> sub-canopy	<i>Corylus avellana</i> , <i>Sorbus aucuparia</i>
Newton Mill (50°52'N, 4°15'W)	25	456	35	NE	<i>Quercus robur</i>	<i>Corylus avellana</i> , <i>Fagus sylvatica</i>
Whitleigh Wood (50°25'N, 4°8'W)	20	1111	27	N	<i>Quercus robur</i> and <i>Betula pendula</i>	<i>Corylus avellana</i> , <i>Fagus sylvatica</i> , <i>Acer pseudoplatanus</i>

776 Table 1. Site descriptions of woodlands used to compare methods for estimating

777 canopy openness. All sites were located in Devon, England.

Method	All seasons		Spring		Summer		Autumn		Winter	
	R ²	p								
Hemispherical photo (ImageJ)	0.96	<0.001	0.85	<0.001	0.77	<0.001	0.94	<0.001	0.69	<0.001
Smartphone fisheye photo (HemiView)	0.89	<0.001	0.83	<0.001	0.67	<0.001	0.79	<0.001	0.05	0.300
Smartphone fisheye photo (ImageJ)	0.84	<0.001	0.74	<0.001	0.76	<0.001	0.66	<0.001	0.08	0.170
Smartphone photo (overhead)	0.85	<0.001	0.57	0.002	0.43	<0.001	0.69	<0.001	0.04	0.380
Smartphone photo (average of 4)	0.81	<0.001	0.15	0.410	0.60	<0.001	0.72	<0.001	0.02	0.490
Canopy scope (overhead)	0.51	<0.001	0.24	0.240	0.01	0.170	0.41	<0.001	0.00	0.820
Canopy scope (largest gap)	0.52	<0.001	0.2	0.029	0.20	0.030	0.33	0.003	0.00	0.850
Canopy scope (average of 4)	0.55	<0.001	0.31	0.005	0.18	0.040	0.55	<0.001	0.00	0.910
Visual estimation (overhead)	0.39	<0.001	0.01	0.740	0.05	0.280	0.31	0.005	0.06	0.260
Visual estimation (average of 4)	0.52	<0.001	0.03	0.460	0.20	0.029	0.51	<0.001	0.04	0.350

778 Table 2. Proportion of variation explained (R^2) and statistical significance (p) for
 779 relationships between hemispherical photography analysed with HemiView and
 780 alternative methods. Relationships were considered separately for each season, as well
 781 as across all seasons together.

Method	Hardwick		Hunshaw		Newton Mill		Whitleigh	
	R²	p	R²	p	R²	p	R²	p
Hemispherical photo (ImageJ)	0.97	<0.001	0.85	<0.001	0.98	<0.001	0.81	<0.001
Smartphone photo fisheye (HemiView)	0.95	<0.001	0.86	<0.001	0.86	<0.001	0.86	<0.001
Smartphone photo fisheye (ImageJ)	0.84	<0.001	0.80	<0.001	0.81	<0.001	0.86	<0.001
Smartphone photo (overhead)	0.88	<0.001	0.78	<0.001	0.68	<0.001	0.85	<0.001
Smartphone photo (average of 4)	0.92	<0.001	0.93	<0.001	0.70	<0.001	0.85	<0.001
Canopy scope (overhead)	0.47	0.002	0.08	0.260	0.68	<0.001	0.19	0.072
Canopy scope (largest gap)	0.42	0.004	0.22	0.049	0.73	<0.001	0.12	0.160
Canopy scope (average of 4)	0.39	0.005	0.25	0.034	0.75	<0.001	0.16	0.100
Visual estimation (overhead)	0.42	0.004	0.1	0.200	0.60	<0.001	0.01	0.630
Visual estimation (average 4)	0.47	0.002	0.2	0.063	0.67	<0.001	0.01	0.740

782 Table 3. Proportion of variation explained (R^2) and statistical significance (p) for
 783 relationships at each woodland site between estimates of canopy openness from
 784 hemispherical photography analysed with HemiView versus estimates from other
 785 methods. Photographs were included from spring, summer and autumn, but not winter.

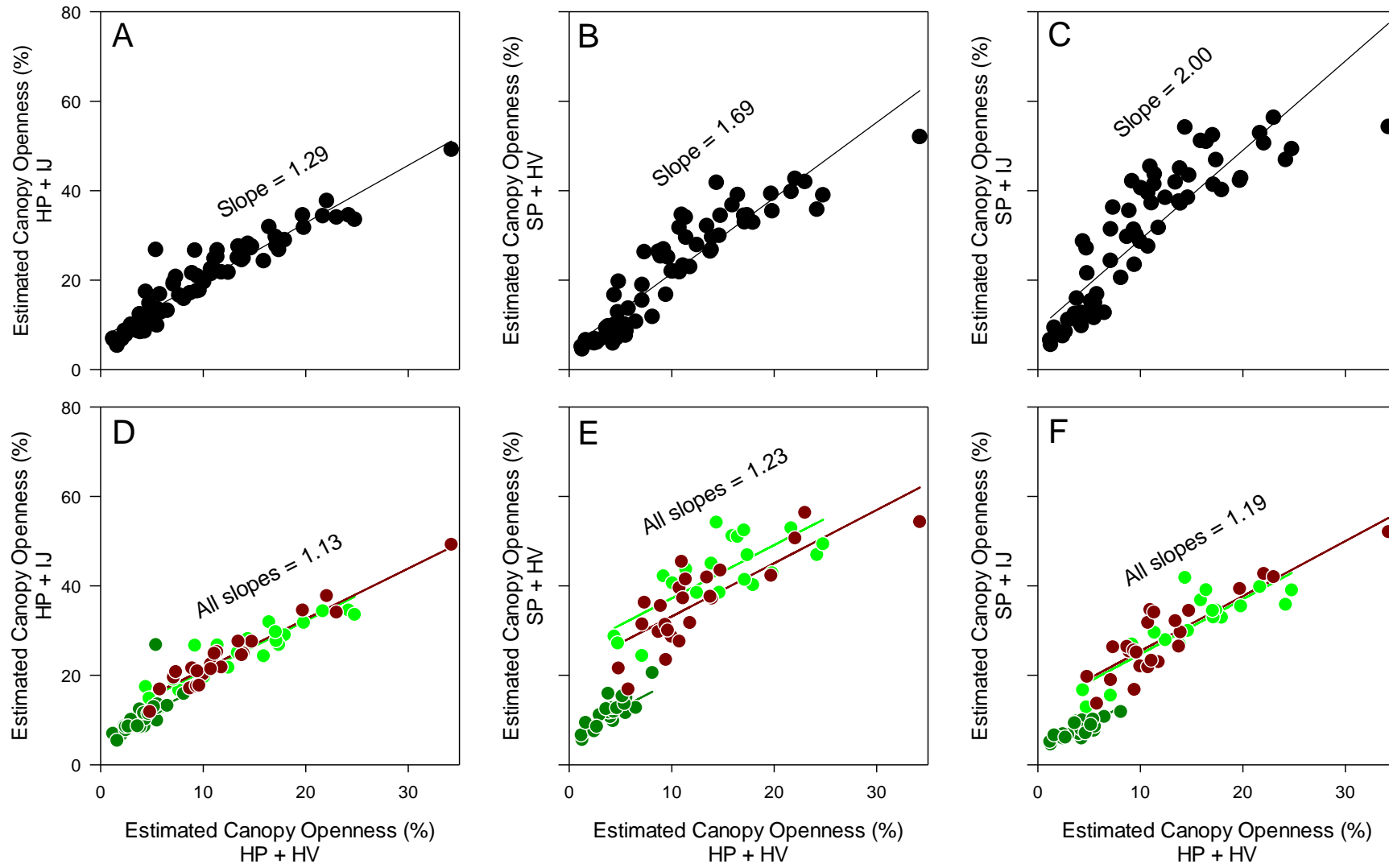
786 **Figures**

787 **Fig. 1.** Canopy openness estimates from hemispherical photography with HemiView
788 (HP+HV) compared with estimates from hemispherical photography with ImageJ
789 (HP+IJ), smartphone fisheye photography with HemiView (SP+HV), and smartphone
790 fisheye photography with ImageJ (SP+IJ). **Figs A–C.** Overall relationships across all
791 seasons. R^2 and statistical significance of these relationships is presented in Table 2.
792 **Figs D–F.** Separate relationships for each growing season (light green = spring, dark
793 green = summer, dark red = autumn).

794 **Fig. 2.** Site canopy openness estimates from hemispherical photography with HemiView
795 (HP+HV) compared with estimates from **(A)** hemispherical photography with ImageJ
796 (HP+IJ), **(B)** smartphone fisheye photography with HemiView (SP+HV), and **(C)**
797 smartphone fisheye photography with ImageJ (SP+IJ). R^2 and statistical significance of
798 these relationships is presented in Table 3. Relationships are shown for each site (red
799 = Hardwick, green = Hunshaw, blue = Newton Mill, grey = Whitleigh).

800 **Fig. 3.** Comparison of estimates of canopy openness using three different models of
801 smartphone in three canopy densities. Every canopy density x phone combination was
802 based on 22 photographs, each taken by a different user. The median is shown as a
803 horizontal line, the box represents values within the 25–75% quartiles, and the error
804 bars show the minimum and maximum values. Means sharing a letter were not
805 significantly different according to *post hoc* contrasts using estimated marginal means.

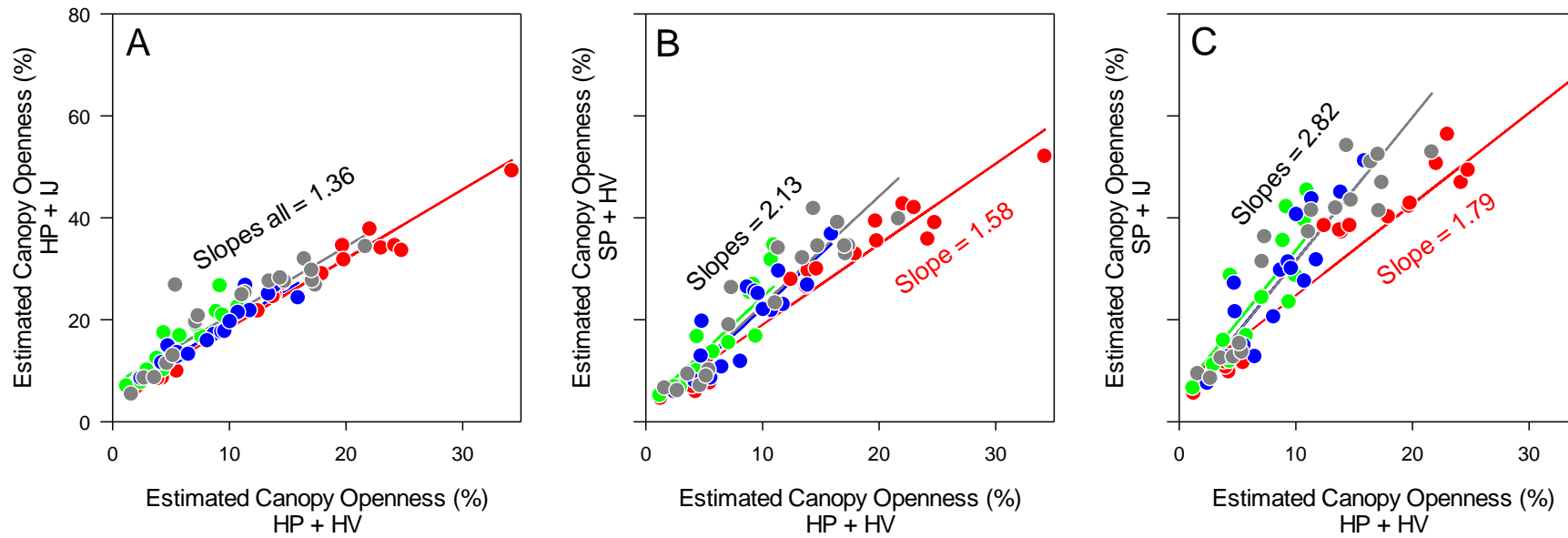
806 Fig. 1



807

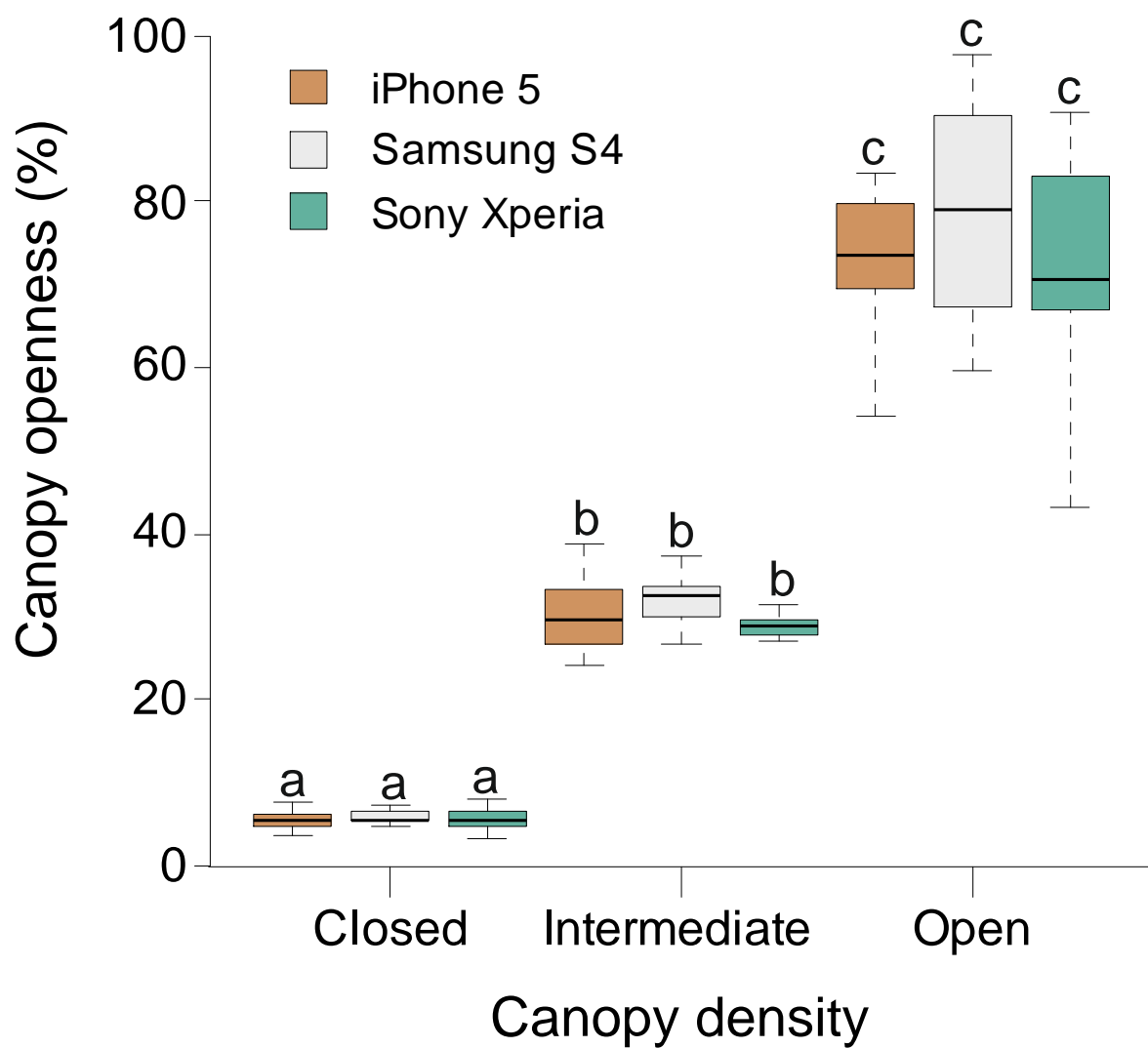
808

809 Fig. 2



810

811 Fig. 3



812